Advanced Journal of Chemistry-Section B
Natural Products and Medical Chemistry

Journal homepage: http://www.ajchem-b.com/

Original Research Article

Synthesis, crystal structure, Hirshfeld surface, crystal voids, energy frameworks, DFT and molecular docking analysis of (2,6-dimethoxyphenyl)acetic acid

Ruchika Sharma[1], Mulveer Singh[1], Kamal[2], Nitin G. Ghatpande[3,4], Mahidansha M. Shaikh[3,4], Jagannath S. Jadhav[5], Saminathan Murugavel[6], and Rajni Kant[1]*

[1]*Chemical Crystallography Laboratory, Department of Physics, University of Jammu, Jammu Tawi-180006, India.*
[2]*Department of Chemistry, Indian Institute of Technology, Jammu, 181221, India.*
[3]*Department of pharmaceutical Chemistry, School of Health Science, University of KwaZulu- Natal, Durban-4041, South Africa.*
[4]*Unique Med Chem Laboratories, L-64, Chincholli MIDC, Solapur-413255, M. S., India.*
[5]*Department of Chemistry, Shivaji University, Kolhapur-416004, M.S., India.*
[6]*Department of Physics, Thanthai Periyar Government Institute of Technology, Vellore-632002, Tamil Nadu, India.*

ARTICLE INFO

Article history
Submitted: 2021-12-17
Revised: 2022-01-17
Accepted: 2022-01-26
Available online: 2022-02-23
Manuscript ID: AJCB-2112-1102
DOI: 10.22034/ajcb.2022.320258.1102

KEYWORDS
Diffraction,
DFT,
Organic synthesis,
Natural products,
pharmaceutical applications.

ABSTRACT

(2,6-dimethoxyphenyl)acetic acid exists in the triclinic crystal system having space group P-1 and lattice dimensions = 7.66(4) Å, b = 8.16(4) Å, c = 8.65(3) Å, V = 503(4) Å^3 and Z = 2. The molecular and crystal structure was elucidated using X-ray crystallographic techniques. The refinement of all the structural parameters was done using the full-matrix least-squares method and it yielded the final R-factor as 0.0579 for 1711 observed reflections. In the crystal packing, molecules are consolidated by intermolecular O-H....O and intramolecular C-H....O interactions. The O-H....O interaction makes a dimer corresponding to $R_2^2(8)$ graph-set motif. Hirshfeld surface (HS) analysis has been complemented to envisage the conformity of the molecular structure. The void-volume analysis has been made to obtain the mechanical strength of the crystal structure. The energy frameworks have been constructed to know the stability of the structure and the kind of dominant energy present in it. The optimized structure using density functional theory (DFT), HOMO–LUMO energy and the charge on the atoms has been examined using B3LYP method. The inhibitory activity of (2,6-dimethoxyphenyl)acetic acid against microbial targets has been assessed using the docking process.

Highlights:

- (2,6-dimethoxyphenyl) acetic acid (DMPAA) has been synthesized by a standard procedure and its three-dimensional structure analyzed using crystallographic techniques.
- The crystal structure has been reinforced by hydrogen bond interactions.
- Hirshfeld surface analysis and DFT calculations have been performed.
- HOMO-LUMO frontier molecular orbitals have been examined (E_{gap} = 5.87 eV)
- Molecular docking of DMPAA with DNA gyrase and CYP51protein has been analyzed and reported.

* Corresponding author: Rajni Kant
✉ E-mail: rkant.ju@gmail.com
☏ Tel number: +91 191 2432051

GRAPHICAL ABSTRACT

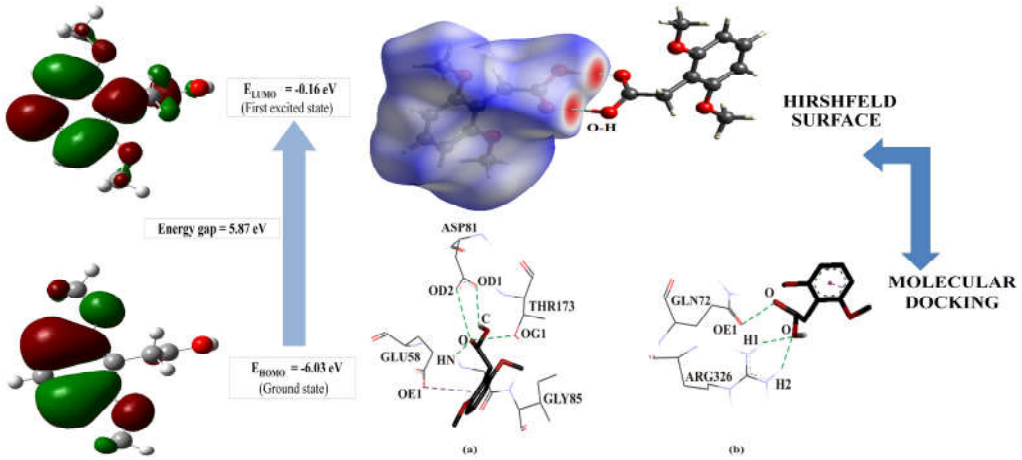

1. Introduction

Compounds derived from substituted phenyl acetic acid are versatile intermediates in synthetic organic chemistry and are broadly used in a range of applications such as in the synthesis of (i) nonsteroidal anti-inflammatory drugs like Ibuprofen and diclofenac [1], (ii) heterocyclic compounds [2] and in many natural products and pharmaceuticals [3]. (2,6-dimethoxyphenyl) acetic acid (DMPAA) is a trifunctional compound with a one carboxylate and two electron rich methoxy functionalities and was obtained by Willgerodt process [4]. It is regio isomer of its other analogue [5] and is an important molecule particularly in relation to neuropsychiatric diseases [6-8]. It is of immense importance for the preparation of 1,2,3,4- tetrahydroiso-quinolines useful for various alkaloidal formulations [9]. The carboxylic acid possesses a diverse structure which can be organised as a centrosymmetric dimer or catemer [10, 11]. The molecular structure of DMPAA was confirmed by single crystal X-ray diffraction studies and other properties, viz. Hirshfeld surface (HS), Crystal voids and Energy frameworks have been carried out using Crystal Explorer (21.5) software [12]. The optimized geometry and Mulliken charges in the ground state were computed using DFT (with B3LYP/6-311G (d, p) basis set). The calculations of the molecule have been performed using Gaussian 09W software [13]. HOMO and LUMO analysis have been performed to extract information about the charge transfer within the molecule. Besides this, some other molecular properties of the optimized structure have also been examined and reported. DNA gyrase play a vital role in biosynthesis of bacterial circular DNA. The blocking of DNA gyrase makes bacterial death [14]. As a result, for the molecular docking studies, it was chosen as the target of an antibacterial agent. Hence, DMPAA was docked with DNA gyrase (PDB id: 3G75) [15]. The obstructing of Lanosterol 14 α-demethylase (CYP51) fights the production of ergosterol in fungi. Without ergosterol, the fungal production is not possible [16]. Owing to this reason, CYP51 was selected as a target for antifungal agent. Thus, DMPAA was docked with CYP51 (PDB id: 1EA1) [17]. Furthermore, the docking results were evaluated using the conventional drugs ciprofloxacin (Bacteria) and fluconazole (fungi), respectively.

2. Materials and methods

2.1. Synthesis and crystallization

The compound was obtained commercially from Sigma Aldrich. The crystallization of DMPAA took place during an attempt to synthesize an ethanone derivative of N-Acyl/aroyl spiro[chromane-2,4-piperidin]-4(3*H*)-one [18]

by reacting 15 mmol of DMPAA with spiro[chromane- 2,4'-piperidin]-4-one (10 mmol) in DCM, followed by sequential addition of Et_3N (30 mmol), DCC (15 mmol), DMAP (5 mol%) and resulting solution was stirred at room temperature for 12 h. The product and unreacted (2,6-dimethoxyphenyl)acetic acid were segregated on quenching, extracting and column purification. The eluent part containing DMPAA was left to slowly evaporate at room temperature over a period of 10 days. Light brown square-type crystals of DMPAA were found on the walls of the test tube. Crystals suitable for the diffraction study were collected during nonreactive substrate attempted in synthesis of N-Acyl/aroyl spiro[chromanr-2,4-piperidin]-4(3*H*)-one. The chemical structure of DMPAA is given in **Fig. 1**.

2.2. Crystal structure and refinement

The diffraction data for a crystal having well defined morphology were collected at 293K by using a Bruker D8 Venture diffractometer.

MoKα – radiation was used (λ = 0.71073 Å) for measuring the reflections in ϕ and ω-scan mode over a range of diffraction angles (2.5 - 26.0°). The data were treated using the standard criteria to obtain 1711 observed reflections. The structure was solved using direct methods (SHELXS97 [19]) and refined by full-matrix least-squares methods using SHELXL97 [20]. All non-H atoms were fixed. The final refinement cycle yielded a final R = 0.0579 and *w*R(F^2) = 0.1553 for 1711 observed reflections.

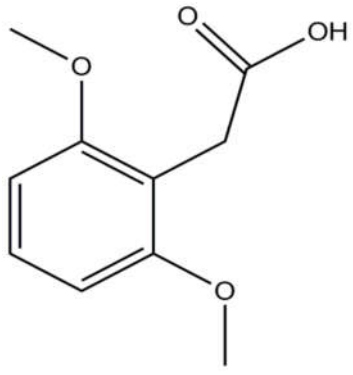

Fig. 1: Chemical Structure of DMPAA.

The atomic scattering coefficients were derived from the International Tables for X-ray Crystallography (1992, Vol. C, Tables 4.2.6.8 and 6.1.1.4) [21]. The crystal data are presented in **Table 1**. The geometry of the molecule was analyzed by using some software, viz. (MERCURY [22], PLATON [23] and PARST [24]).

2.3. Computational details

The HS plots, crystal voids and energy frameworks were computed using the Crystal Explorer (21.5) software [12]. The Hartree Fock (HF) and DFT methods were used to optimize the structure of DMPAA (using Gaussian 09W [13]) with standard B3LYP/6-311G (d, p) basis sets. The atomic coordinates were imported into Crystal Explorer (21.5) and Gaussian 09W software from the approved CIF. Molecular docking simulation mock-ups were performed using AutoDock Vina software [25]. The 3D crystal structure of DNA gyrase and CYP51 were imported from Protein Data Bank (PDB ID: 3g75 and 1EA1). The coordination of the grid box positioned at X= 51.19, Y = -3.99, Z = 17.94 (for DNA gyrase) and X = -17.28, Y = -7.28, Z = 63.72 (for CYP51) for docking analysis. Out of ten conformations attained, the prominent conformation was picked based on the binding score. One of the fine affinities binded at the active site was visualised using Discover Studio Visualizer.

3. Results and discussion

3.1. Crystal structure description of (2,6-dimethoxyphenyl)acetic acid

The bond geometry is presented in **Table 2. Fig. 2** is an ORTEP image of DMPAA with usual atomic numbering. The bond distances and angles of the benzene ring are within the usual range [26] and these parameters are comparable with some analogous structures [27, 28]. The acetic acid substituent is almost held at right angle to the benzene ring (the dihedral angle between the two is 89.54°).

Table 1. Crystal and structure-refinement data for $C_{10}H_{12}O_4$.

CCDC number	2105160
Chemical formula	$C_{10}H_{12}O_4$
M_r	196.20
Crystal system, space group	Triclinic, P-1
Temperature (K)	293(2)
a, *b*, *c* (Å)	7.66(4), 8.16(4), 8.65(3)
α, β, γ (°)	98.22(11), 106.02(13),98.98(13)
V (Å^3)	503(4)
Z	2
Radiation type	Mo *K*α
μ (mm^{-1})	0.100
2θ range for data collection	2.50°- 26.00°
Sample size (mm)	0.40 x 0.30 x 0.20
No. of measured, independent and observed [I> 2σ(*I*)] reflections	21337, 1938, 1711
R_{int}	0.069
$R[F^2 > 2\sigma(F^2)]$, $wR(F^2)$, *S*	0.0579, 0.1553, 1.095
No. of reflections	1711
No. of parameters	130
h, k, l	-9 to 9, -10 to 10, -10 to 10
$\Delta\rho_{max}$, $\Delta\rho_{min}$ (e Å^{-3})	0.282, -0.254

The expansion and contraction in the bond angles at C6 (124°) and C2 (115°), respectively, is primarily due to the repulsive interaction between methyl carbons (C7 and C10) with the six-membered ring. Molecules in the crystal are integrated via the combination of a sole O2-H2....O3 intermolecular interaction and C8-H8A....O1 intramolecular interaction (Table 3). The O2-H2....O3 interaction leads to the formation of a dimer (**Fig. 3**) that corresponds to the R_2^2 (8) graph-set pattern. Fig. 4 depicts the packing arrangement of molecules in the unit cell [22].

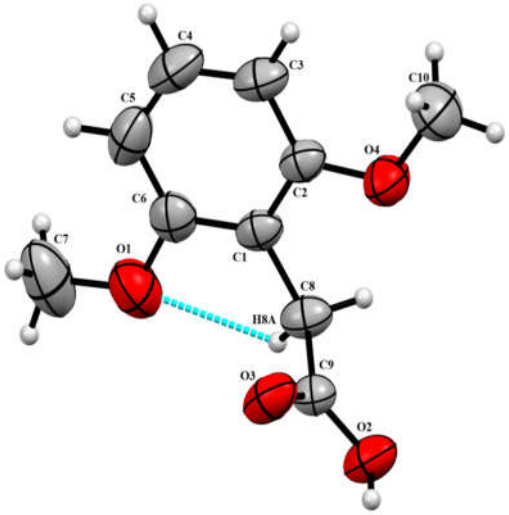

Fig. 2: Thermal ellipsoidal plot for DMPAA.

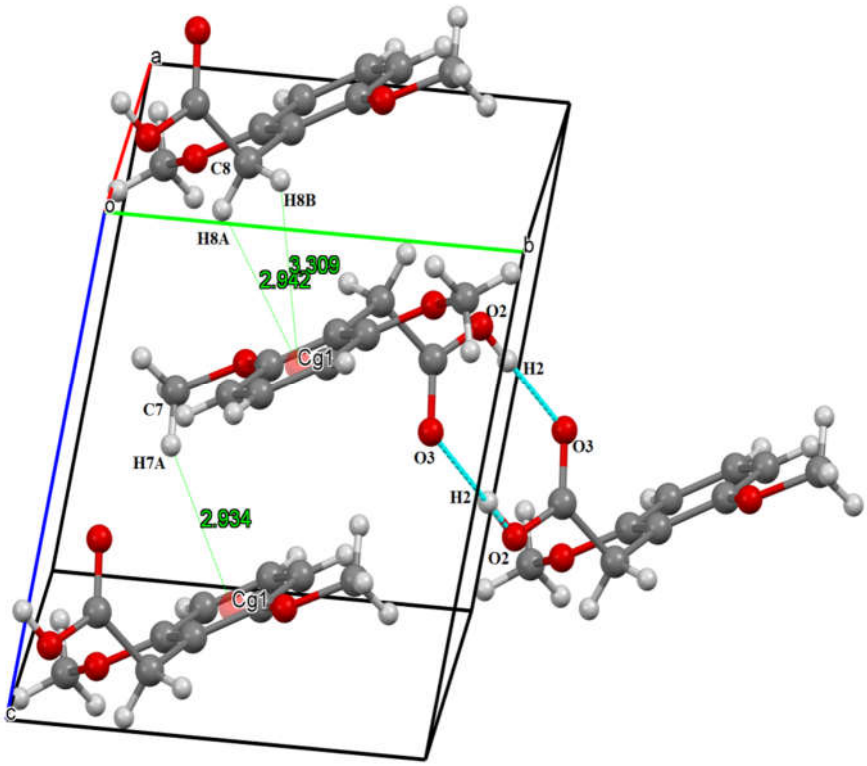

Fig. 3: Representative dimer with R_2^2 (8) graph-set motif (a-axis).

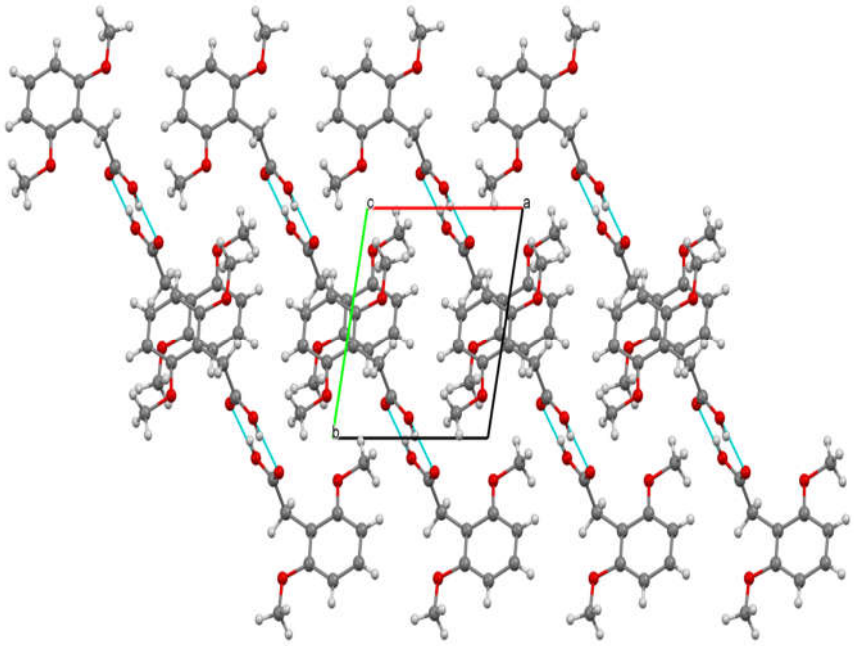

Fig. 4: The packing arrangement of DMPAA in the unit cell.

Table 2. Selected (comparative) experimental and calculated geometric parameters (Å, °).

Parameters	**Experimental**	**Calculated**	
Bond Lengths	**XRD data**	**HF/6-311G (d, p)**	**DFT/6-311G (d, p)**
O1-C6	1.364(6)	1.346	1.366
O2-C9	1.289(5)	1.333	1.359
O3-C9	1.231(5)	1.180	1.201
O4-C2	1.366(6)	1.346	1.366
C1-C6	1.390(6)	1.390	1.401
C1-C2	1.390(6)	1.390	1.390
C2-C3	1.387(7)	1.389	1.398
C3-C4	1.370(6)	1.380	1.390
C4-C5	1.375(6)	1.380	1.390
C5-C6	1.392(7)	1.389	1.398
Bond Angles			
C2-O4-C10	118.8(3)	120.3	118.8
O4-C2-C3	124.1(2)	123.5	123.8
O4-C2-C1	115.2(3)	115.5	115.1
C1-C2-C3	120.7(4)	121.0	121.0
C2-C1-C6	119.0(3)	118.7	118.5
C2-C1-C8	119.5(4)	120.6	120.7
C6-C1-C8	121.5(2)	120.6	120.7
C1-C8-C9	114.5(3)	113.9	113.7
O1-C6-C1	115.2(3)	115.5	115.2
O1-C6-C5	124.0(4)	123.5	123.8
C1-C6-C5	120.8(2)	121.0	121.0
O3-C9-O2	122.8(2)	122.1	122.4
O3-C9-C8	123.3(3)	127.1	127.3
O2-C9-C8	113.9(3)	110.7	110.3
C6-O1-C7	118.4(3)	120.3	118.8
C9-O2-H2	109.5	108.0	106.1
Torsion Angles			
C7-O1-C6-C1	-177.9(2)	-177.0	-179.1
C10-O4-C2-C1	176.2(1)	176.2	179.0
C6-C1-C8-C9	-96.9(4)	-89.6	-89.6
C2-C1-C8-C9	83.3(4)	89.5	89.6

Table 3. Hydrogen-bond geometry (Å, °)

D–H···A	**D–H**	**H···A**	**D···A**	**D–H···A**
O2–H2···O3^{i}	0.82	1.84	2.654	170.0
C8–H8A···O1	0.97	2.36	2.754	104.0
C7–H7A···Cg1^{ii}	0.96	2.934	3.791	149.3
C8–H8A···Cg1^{iii}	0.97	2.942	3.516	119.0
C8–H8B···Cg1^{iii}	0.97	3.309	3.516	94.22

Symmetry code: (i) 2-x, 2-y, 1-z (ii) -x, 1-y, 1-z (iii) -x, 1-y, -z
Cg1 denotes the centre of gravity for a six-membered ring .

3.2 Hirshfeld surface and 2D fingerprint plot analysis

The HS and their respective 2D fingerprint plots were generated using Crystal Explorer 21.5 and the intermolecular interactions in the crystal packing were quantified and decoded using d_{norm} (normalized contact distance) and 2D fingerprint plots, respectively. The short interatomic contacts are shown as dark red spots while the other intermolecular interactions exist as light-red spots. The d_i (inside) and d_e (outside) illustrates the distances to the HS from the nuclei, with respect to the relative van der Waal's radii. The relative contribution of the contacts over the surface is visualized through the colour gradient (blue to red) in the 2D fingerprint plots. The HS of DMPAA mapped over d_{norm} in the range -0.7228 to 1.3703 a.u. is shown in Fig. 5. The red spots corresponding to H...O contacts are due to the existence of O-H...O hydrogen bonds. The white areas represent H...H interactions and correspond to the places where the distances separating neighbouring atoms are close to the sum of the van der Waals radii of the reference atoms. The bluish region indicates areas where neighbouring atoms are too far apart, for there to be no interactions between them.

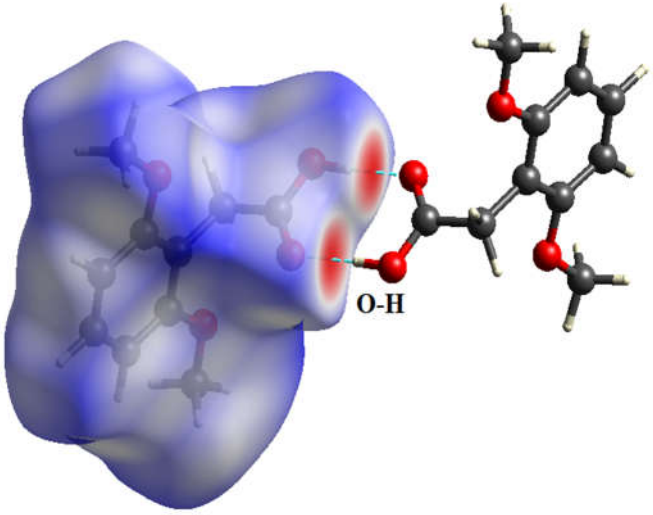

Fig. 5: Depicting Hirshfeld surface map

.

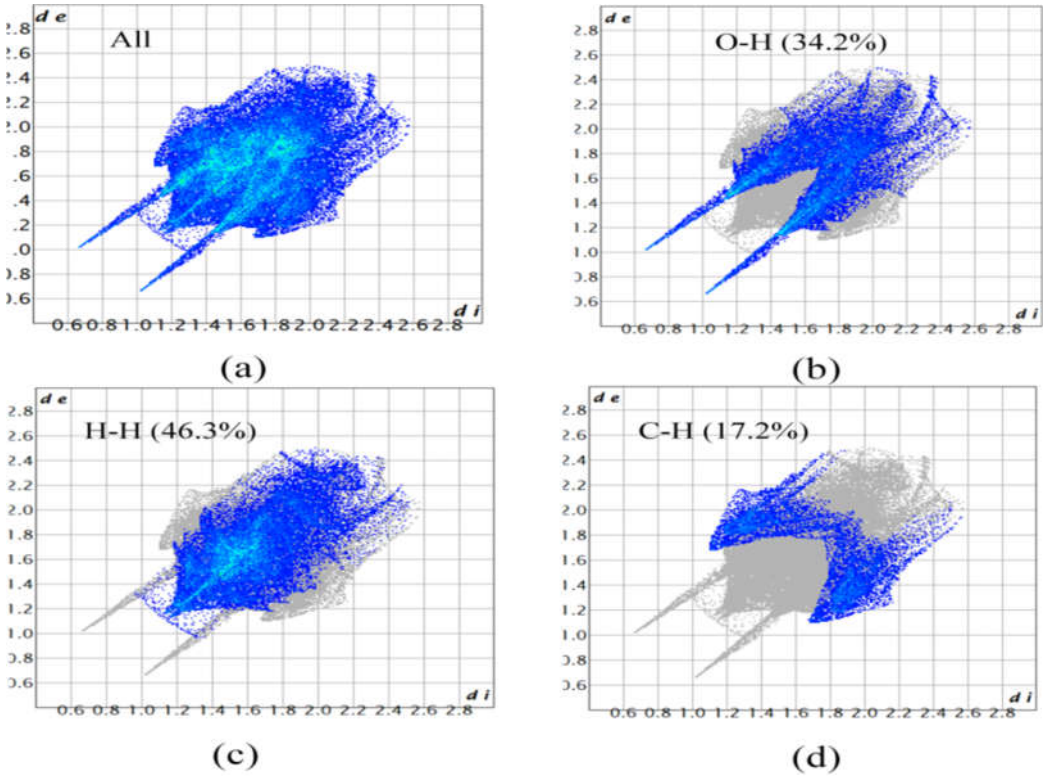

Fig. 6: Two-dimensional fingerprint plots.

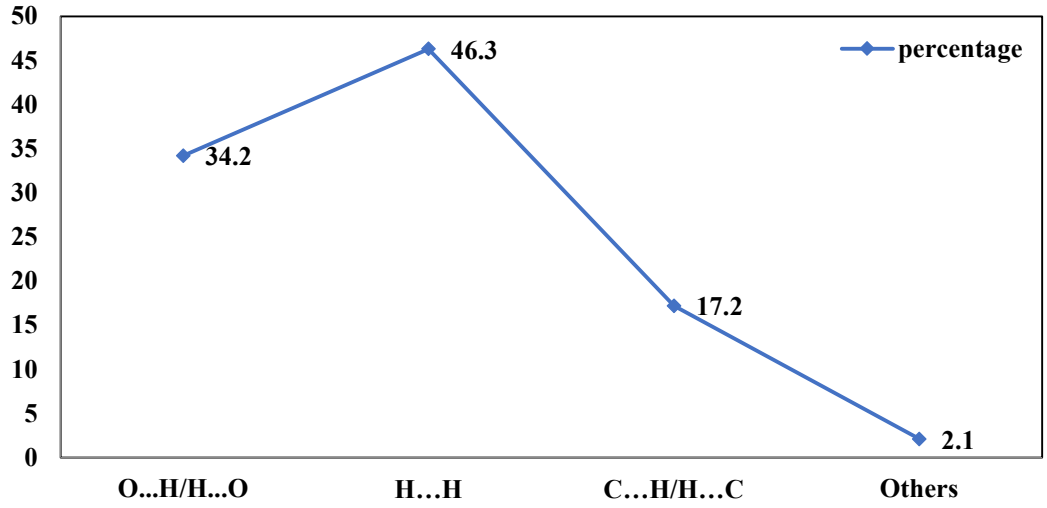

Fig. 7: Relative contribution of various intermolecular interactions to the Hirshfeld surface area.

The percentage of intermolecular interactions as obtained from the 2D fingerprint plots is: H...H (46.3%), O-H/H-O (34.2%) and C-H/H-C (17.2%). The overall contribution of O...H contacts (34.2%) is represented by two symmetrical spikes [**Fig. 6(b)]** while the H...H interactions (46.3%) of the entire surface is represented by one spike [**Fig. 6(c)**]. A graphical representation of the interactions contribution as obtained from the fingerprint plots is shown in **Fig. 7**.

3.2.1. Shape Index and Curvedness Map

Fig. 8(a) shows the molecular HS mapped over the shape index of DMPAA indicating the touch points for the pairs of red and blue colour regions [29]. Hydrogen-acceptor groups constitute the concave red regions on the shape index surface, while the surface around the donor atoms i.e. hydrogen-donor groups is highlighted as blue bumps region. The near absence of adjacent red and blue triangles clearly shows the non-occurrence of π-π interactions (**Fig. 8(a)**). The **Fig. 8(b)** illustrates the mapping over the curvedness of the molecule which shows large green areas separated by dark blue curves thus; there are no flat patches on the surface and no planar stacking present between the molecules.

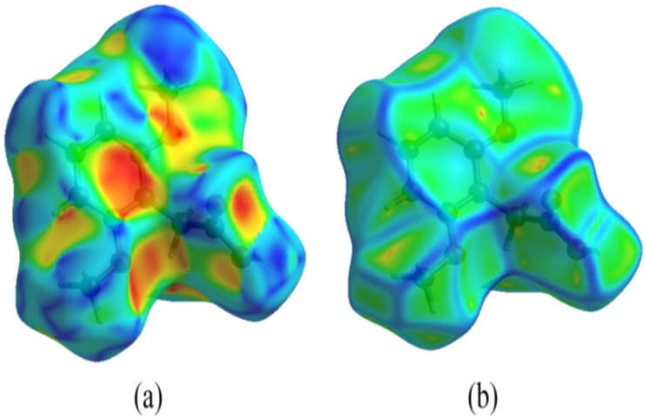

Fig. 8: (a) Shape index plot mapped over HS (b) Curvedness plot (indicating the non- planar stacking of the molecules).

3.2.2. Crystal voids

The voids in the crystal structure of DMPAA as shown in **Fig. 9** have been detected by constructing a (0.002 au) - isosurface of procrystal electron density which used to find the empty space in a crystal by determining the shape and size of the molecules. This gives the void volume as 67.07 $Å^3$ and with unit cell volume of 503 $Å^3$ [**Table 1**], the estimated void volume of DMPAA comes out to be 13.3 % of the unit cell volume with no large cavities.

3.3. Energy Frameworks

The interaction energies were used to construct the 3D topology of interactions (termed as energy frameworks) using Crystal Explorer 21.5. These were computed through a single point molecular wave function calculated at the B3LYP/6-311 G(d,p) level. The total interaction energy around the reference molecule (3.8 Å radius cluster) indicates the dominance of dispersion energy (-175.7 kJ/mol) over the electrostatic (-165.3 kJ/mol) and polarization energy components (-44.5 kJ/mol), respectively.

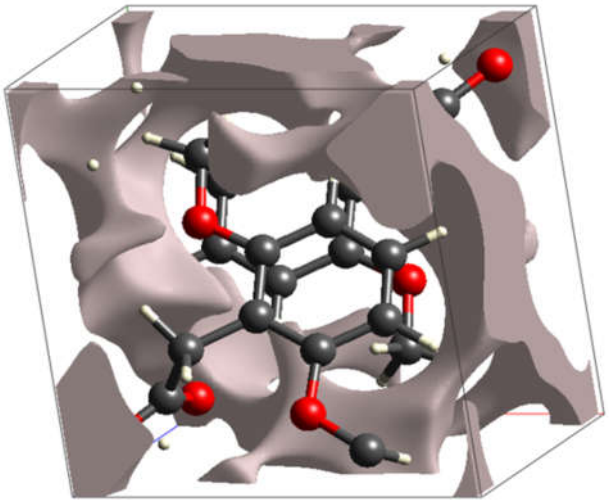

Fig. 9: Unit cell void (0.002 au) – isosurface.

Table 4. Different interaction energies of the molecules pairs in kJ/mol [electron density B3LYP/6-31G (d,p)].

	N	Symop	R	E_ele	E_pol	E_dis	E_rep	E_tot
	1	-x, -y, -z	8.04	-123.9	-29.1	-13.4	145.1	-74.5
	2	x, y, z	10.28	1.1	-0.2	-2.2	0.1	-0.8
	1	-x, -y, -z	7.81	-0.3	-1.0	-10.5	3.9	-7.8
	2	x, y, z	8.16	-4.4	-1.4	-13.7	6.2	-13.8
	2	x, y, z	7.66	-3.8	-0.7	-14.1	9.1	-11.2
	1	-x, -y, -z	7.86	-8.0	-1.2	-18.2	12.2	-17.7
	1	-x, -y, -z	5.37	-18.8	-8.9	-39.9	29.4	-43.0
	1	-x, -y, -z	4.29	-4.3	-1.5	-48.5	22.5	-33.9
	1	-x, -y, -z	8.18	-2.9	-0.5	-15.2	10.8	-10.0

The scale factors used are: k_ele = 1.057, k_pol = 0.740, k_disp = 0.871 k_rep = 0.618 [30].

The overall interaction energy is -212.7 kJ/mol. The 3D energy frameworks are depicted in Fig. 10, which shows different interaction energies through the tube size. The tube in the energy frameworks determines the strength of molecular packing in various directions. Interaction energies with order of magnitude less than a certain threshold can be neglected while generating the energy frameworks.

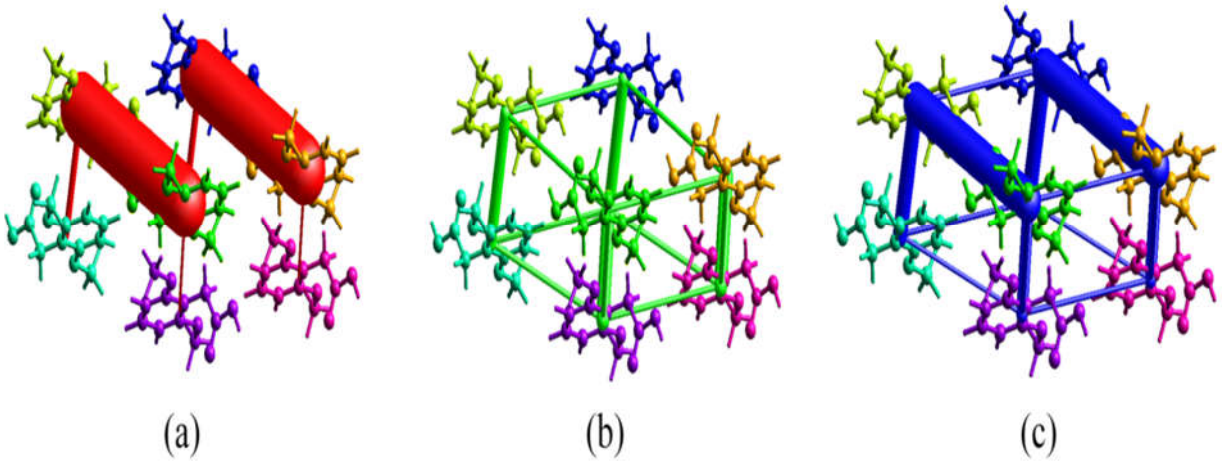

Fig. 10: The graphical representation of coulomb interaction energy (red), dispersion energy (green) and total interaction energy (blue) of DMPAA along b-axis.

3.4. Molecular geometry

The optimized structure of DMPAA is shown in Fig. 11. A comparison of the calculated and observed values shows some variation particularly in bond distances (Table 2). There is some expected variation in the bond angle at C9 position of the acetic acid group. The global minimum energy obtained for the optimized structure is -685.28879650 au and -689.36690737 au, respectively, the difference being -4.08 au.

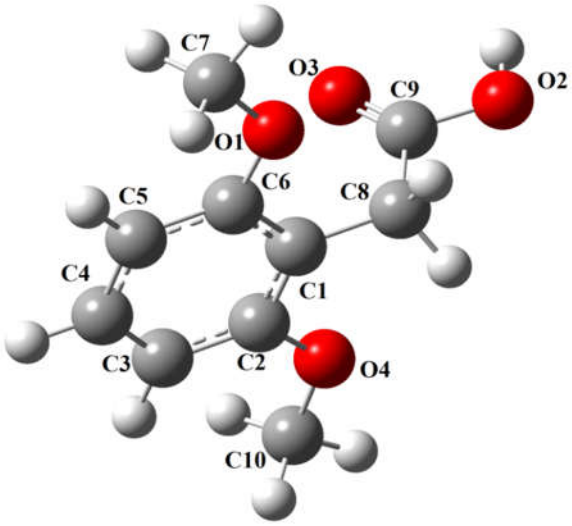

Fig. 11: Optimized structure of DMPAA.

3.5. Atomic Mulliken charge

Mulliken atomic charge calculation plays a significant role in the application of quantum chemical calculation to molecular systems [31]. It is related to the vibrational characteristics of the molecule and helps us know how the electronic structure changes as atomic displacement occur and is connected on to the chemical bonds of the molecule. The parameters like dipole moment, polarizability and reactivity, rely on the atomic charges of the molecular systems. The Mulliken atomic charges for DMPAA as calculated by HF/B3LYP and DFT/B3LYP methods using 6-311G (d,p) basis set are given in Table 5 and their plot is shown in Fig. 12. There is some excessive charge delocalization in the molecule and it is evident from the negative and positive charge on atoms O4 and C9, respectively. All hydrogen atoms show positive Mulliken charge values. The range of hydrogen atom charge in case of HF/6-311G (d,p) is 0.089 - 0.266, while the range of hydrogen atom charges in case of B3LYP/6-311G (d,p) is 0.091 - 0.224. The atom O3 possessing a negative charge plays its role in the formation of O2-H2….O3 intermolecular interaction.

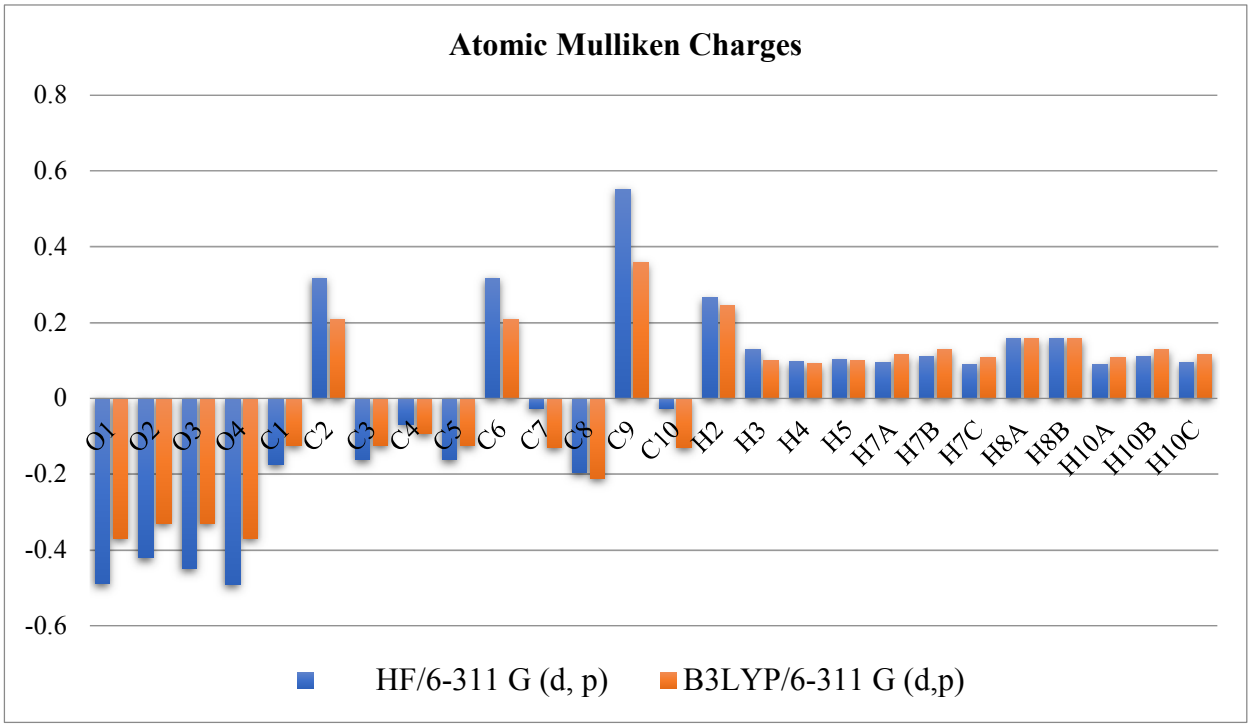

Fig. 12: Mulliken population analysis of DMPAA.

Table 5. Atomic charges for optimized geometry of (2,6-dimethoxyphenyl)acetic acid.

Atom no.	HF/6-311 G (d, p)	B3LYP/6-311 G (d, p)
O1	-0.489	-0.368
O2	-0.421	-0.330
O3	-0.448	-0.330
O4	-0.490	-0.368
C1	-0.175	-0.124
C2	0.318	0.209
C3	-0.162	-0.124
C4	-0.068	-0.093
C5	-0.162	-0.124
C6	0.318	0.209
C7	-0.027	-0.130
C8	-0.195	-0.210
C9	0.551	0.358
C10	-0.027	-0.130
H2	0.266	0.244
H3	0.130	0.099
H4	0.097	0.091
H5	0.104	0.099
H7A	0.095	0.115
H7B	0.111	0.128
H7C	0.089	0.109
H8A	0.159	0.158
H8B	0.159	0.158
H10A	0.089	0.109
H10B	0.111	0.128
H10C	0.095	0.115

3.6. Frontier molecular orbital analysis

The frontier molecular orbitals (LUMO and HOMO) represent the ability to obtain and donate an electron within the molecule. The HOMO orbital is located at -6.03 eV over the entire molecule while the LUMO orbital is at -0.16eV (Fig. 13). The energy difference between these two orbitals is 5.87 eV and it plays an important role in the kinetic stability of the molecule and also shows charge transfer from an electron donor to the electron acceptor group within the molecule. A large value of energy gap between the molecular orbitals is related with the high kinetic stability [32]. If the energy gap between HOMO and LUMO is small, the molecule will be more reactive. All global reactivity parameters are given in Table 6.

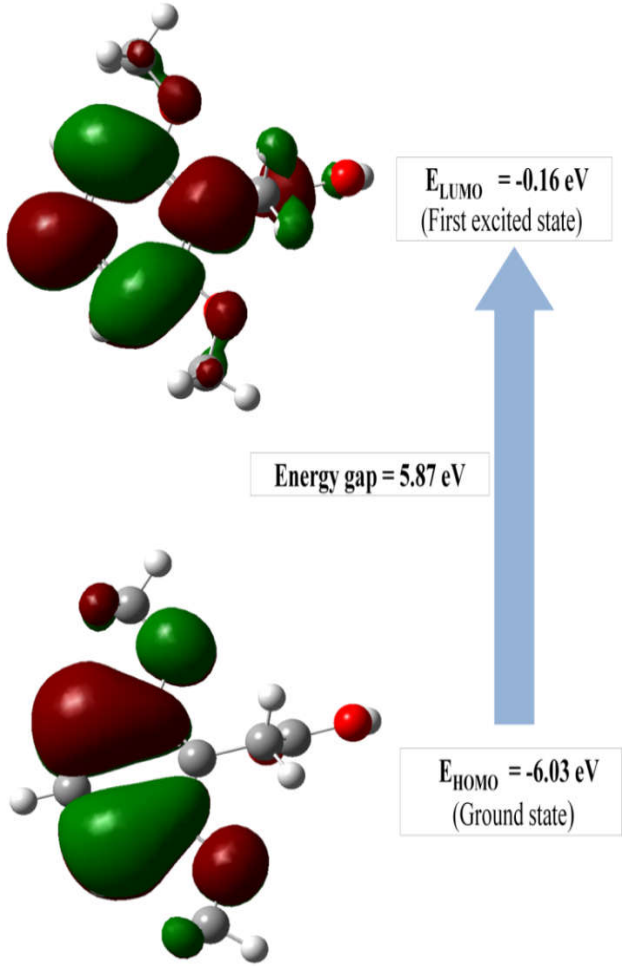

Fig. 13. Frontier molecular orbitals of DMPAA.

Table 6. HOMO-LUMO and other related molecular properties of (2,6-dimethoxyphenyl) acetic acid.

Molecular parameters (eV) B3LYP/6-311G(d,p)	
E_{LUMO}	-0.16
E_{HOMO}	-6.03
$E_{LUMO} - E_{HOMO}$	5.87
Ionization potential (I)	6.03
Electron affinity (A)	0.16
Global hardness (η)	2.93
Chemical potential (μ)	-3.09
Electronegativity (ϰ)	3.09
Global electrophilicity (ω)	1.63
Dipole moment	1.52

3.7. Molecular docking analysis

The (2,6-dimethoxyphenyl)acetic acid - DNA gyrase complex consists of hydrogen interactions with residue GLY85, ASP81 and THR173 and electrostatic interaction with residue GLU58 are shown in Fig. 14(a). The binding energy, bond length and bonding type of interaction in complex DMPAA-DNA gyrase complex are given in Table 7. The docking outcome suggests that binding energy of DMPAA-DNA gyrase complex (-5.1 kcal m^{-1}) is higher as compared to that of Ciprofloxacin-DNA gyrase complex (-4.01 kcal m^{-1}) [33].

The DMPAA -CYP51 complex consists of hydrogen interactions with residue ARG326 and GLN72 are shown in Fig. 14(b) and the binding energy, bond length and bonding type of interaction in complex DMPAA-CYP51is presented in Table 7. The binding energy of DMPAA-CYP51 complex (-5.6 kcal m^{-1}) comes out to be better than that of Fluconazole - CYP51 (-3.59 kcal m^{-1}) [33]. From Table 7, DMPAA display strong attraction with the targets (DNA gyrase/CYP51) and also have high docking energy than the standard drugs (Ciprofloxacin and Fluconazole). Hence, DMPAA may act as a useful anti-microbial drug.

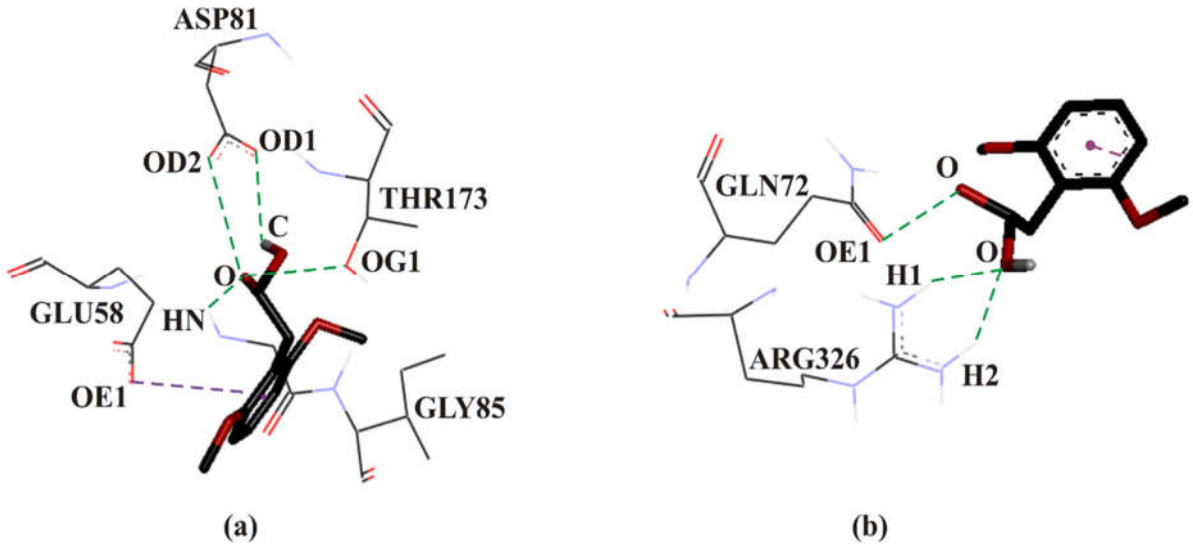

Fig. 14: Molecular interaction of (2,6-dimethoxyphenyl)acetic acid with (a) DNA gyrase and (b) CYP51 binding site.

Table 7. Binding energy, hydrogen bonds of (2,6-dimethoxyphenyl)acetic acid with DNA gyrase and CYP51.

Complex*	Binding Energy (Kcal m^{-1})	Interactions	Distance Å	Bonding	Bonding Types
1	**5.1**	GLY85[HN…O]	2.2852	Hydrogen	H-bond
		[O…OD2]ASP81	3.2860	Hydrogen	H-bond
		[O…OG1]THR173	3.0101	Hydrogen	H-bond
		[CH…OD1]ASP81	2.6493	Hydrogen	H-bond
		GLU58 [OE1…π]	3.9290	Electrostatic	Pi-Anion
2	**5.6**	ARG326[H1…O]	2.0619	Hydrogen	H-bond
		ARG326[H2…O]	2.0992	Hydrogen	H-bond
		[O…OE1]GLN72	3.2144	Hydrogen	H-bond

*1 = (2,6-dimethoxyphenyl)acetic acid +3G75
2 = (2,6-dimethoxyphenyl)acetic acid +CYP51

4. Conclusions

The structure exists in triclinic system with space group P-1. The acetic acid group is held almost at right angle to the benzene ring. Hydrogen-bond analysis shows that molecules are packed through intermolecular O-H....O bond which makes a dimer with graph-set motif $R_2^2(8)$. The HS and 2D fingerprint plots were employed to investigate intermolecular interactions in the crystal structure of DMPAA. The contribution of H-H contacts (46.3%) is significant. The void volume in the unit cell is small and hence reveals the absence of any large cavity. The three-dimensional interaction energy analysis shows that the dispersion energy frameworks dominate the classical electrostatic terms. The molecular structure and other related properties have been investigated using DFT theory. The large value of HOMO-LUMO energy gap (5.87 eV) indicates low chemical reactivity and high kinetic stability of

the molecule. The docking study suggests that the DMPAA possesses greater binding affinity when compared with standard drugs (Ciprofloxacin and Fluconazole) and carries the potential to act as an anti-microbial drug.

Acknowledgement

Rajni Kant is thankful to the University of Jammu for funding under the RUSA- 2.0 project of the Government of India.

References

[1] C. Castellari, and S. Ottani, Anti-Inflammatory Drugs. II. Salt of 2-(2,6-Dichlorophenylamino) phenylacetic Acid with Diethanolamine. *Acta Crystallographica,* C51 (1995) 2612-2615.

[2] P.P. Deshpande, V.B. Nanduri, A. Pullockaran, H. Christie, R.H. Mueller and R.N. Patel, Microbial hydroxylation of o-bromophenylacetic acid: synthesis of 4-substituted-2,3-dihydrobenzofurans. *Journal of Industrial Microbiology and Biotechnology*, 35 (2008) 901–906.

[3] J.J. Jackson, H. Kobayashi, S.D. Steffens and A. Zakarian, 10-Step Asymmetric Total Synthesis and Stereochemical Elucidation of (+)-Dragmacidin D. *Angewandte Chemie International Edition*, 54 (2015) 9971-9975.

[4] D.L. Priebbenow and C. Bolm, Recent advances in the Willgerodt–Kindler reaction. *Chemical Society Reviews,* 42 (2013) 7870-7880.

[5] B. Hachuła, M. Nowak and J. Kusz, Hydrogen-bonding interactions in (3, 4-dimethoxyphenyl) acetic acid monohydrate. *Acta Crystallographica,* C64 (2008) o357–o360.

[6] A.J. Friedhoff and E.Van Winkle, Isolation and Characterization of a Compound from the Urine of Schizophrenics. *Nature (London)*, 194 (1962a) 897–898.

[7] A.J. Friedhoff and E. Van Winkle , The characteristics of an amine found in the urine of Schizophrenic patients. *The Journal of Nervous and Mental Disease,* 135 (1962b) 550–555.

[8] A. Barbeau, J.A. De Groot, J.G. Joly, D.R. Tremblay and J. Donaldson, Urinary excretion of a 3-4, dimethoxyphenylethylamine-like substance in Parkinson's disease. *Revue Canadienne de Biologie,* 22 (1963) 469–472.

[9] J. Szawkało and Z. Czarnocki, Enantioselective Synthesis of Some Tetracyclic Isoquinoline Alkaloids by Asymmetric Transfer Hydrogenation Catalysed by a Chiral Ruthenium Complex. *Monatshefte für Chemie*, 136 (2005) 1619–1627.

[10] L. Leiserowitz, Molecular packing modes. Carboxylic acids. *Acta Crystallographica,* B32 (1976) 775–802.

[11] D. Das and G.R. Desiraju, Packing Modes in Some Mono- and Disubstituted Phenylpropiolic Acids: Repeated Occurrence of the Rare *syn,anti* Catemer. *Chemistry, an Asian Journal,* 1–2 (2006) 231–244.

[12] P.R. Spackman, M.J. Turner, J.J. McKinnon, S.K. Wolff, D.J. Grimwood, D. Jayatilaka and M.A. Spackman. CrystalExplorer: a program for Hirshfeld surface analysis, visualization and quantitative analysis of molecular crystals. Journal of Applied Crystallography 54 (2021) 1006-1011.

[13] M.J. Frisch, G.W. Trucks, H.B. Schlegel, G.E. Scuseria, M.A. Robb, J.R. Cheeseman, G. Scalmani, V. Barone, B. Mennucci, G.A. Petersson, H. Nakatsuji, M. Caricato, X. Li, H.P. Hratchian, A.F. Izmaylov, J. Bloino, G. Zheng, J.L. Sonnenberg, M. Hada, M. Ehara, K. Toyota, R. Fukuda, J. Hasegawa, M. Ishida, T. Nakajima, Y. Honda, O. Kitao, H. Nakai, T. Vreven, J.A. Montgomery Jr., J.E. Peralta, F. Ogliaro, M. Bearpark, J.J. Heyd, E. Brothers, K.N. Kudin, V.N. Staroverov, R. Kobayashi, J. Normand, K.

Raghavachari, A. Rendell, J.C. Burant, S.S. Iyengar, J. Tomasi, M. Cossi, N. Rega, J.M. Millam, M. Klene, J.E. Knox, J.B. Cross, V. Bakken, C. Adamo, J. Jaramillo, R. Gomperts, R.E. Stratmann, O. Yazyev, A.J. Austin, R. Cammi, C. Pomelli, J.W. Ochterski, R.L. Martin, K. Morokuma, V.G. Zakrzewski, G.A. Voth, P. Salvador, J.J. Dannenberg, S. Dapprich, A.D. Daniels, O. Farkas, J.B. Foresman, J.V. Ortiz, J. Cioslowski and D.J. Fox, Gaussian 09, Revision A.1, Gaussian, Inc., Wallingford, CT. 2013.

[14] A. Wehenkel, P. Fernandez, M. Bellinzoni, V. Catherinot, N. Barilone, G. Labesse,M. Jackson and P.M. Alzari, The structure of PknB in complex with mitoxantrone, an ATP-competitive inhibitor, suggests a mode of protein kinase regulation in mycobacteria. *FEBS Letters,* 580 (2006) 3018-3022.

[15] N. Aoumeur, N. Tchouar, S. Belaidi, M. Ouassaf, T. Lanez and S. Chtita, Molecular docking studies for the identifications of novel antimicrobial compounds targeting of staphylococcus aureus. *Moroccan Journal of Chemistry*, 9(2) (2021) 274-289.

[16] S.M. El-Feky, L.A. Abou-Zeid, M.A. Massoud, S.G. Shokralla1 and H.M. Eisa, Computational Design, Molecular Modeling and Synthesis of New 1,2,4 – Triazole Analogs with Potential Antifungal Activities. *SMU Medical Journal*, 1(2) (2014) 224-242.

[17] T. Jorda and S. Puig, Regulation of Ergosterol Biosynthesis in Saccharomyces cerevisiae. *Genes,* 11 (2020) 795.

[18] A.R. Shinde and D.B. Muley. Synthesis, Characterization and Evaluation of Antioxidant and Antimicrobial activity of Spirochromones Derivatives. *Anti-Infective Agents,* 18 (2020) 352 - 361.

[19] G.M. Sheldrick, A Short History of SHELX. *Acta Crystallographica,* A64, (2008) 112-122.

[20] G.M. Sheldrick, *SHELXT* – Integrated space-group and crystal-structure determination. *Acta Crystallographica,* C71 (2015) 3-8.

[21] A.J.C. Wilson, International Tables for Crystallography Volume C: Mathematical, Physical and Chemical Tables. *Acta Crystallographica, A51 (1995) 441-444.*

[22] C.F. Macrae, I.J. Bruno, J.A. Chisholm, P.R. Edgington, P. McCabe, E. Pidcock, L. Rodriguez-Monge, R. Taylor, J. Van De Streek, and P.A. Wood, New Features for the Visualization and Investigation of Crystal Structures. *Journal of Applied* Crystallography, 41 (2008) 466-470.

[23] A.L. Spek, Structure validation in chemical crystallography. *Acta Crystallographica,* D65 (2009) 148-155.

[24] M. Nardelli, PARST: a system of Fortran routines for calculating molecular structure parameters from the results of crystal structure analyses. *Journal of Applied* Crystallography, 28 (1995) 659-659.

[25] O. Trott and A.J. Olson, AutoDock Vina: improving the speed and accuracy of docking with a new scoring function, efficient optimization and multithreading. *Journal of Computational Chemistry*, 31 (2010) 455-461.

[26] F.H. Allen, O. Kennard, D.G. Watson, L. Brammer, A.G. Orpen and R.J. Taylor. Tables of Bond Lengths determined by X-Ray and Neutron Diffraction. Part I. Bond Lengths in Organic Compounds. *Journal of the Chemical Society, Perkin Transactions 2*, 2 (1987) 1-19.

[27] B. Hachula, M. Nowak and J. Kusz, Hydrogen-bonding interactions in (3,4-dimethoxyphen-

yl)acetic acid monohydrate. *Acta Crystallographica*, C64 (2008) o357-o360.

[28] D. Chopra, A.R. Choudhury and T.N. Guru Row, 3, 4-Dimethoxyphenylacetic acid. *Acta Crystallographica,* E59 (2003) o433-o434.

[29] M.J. Turner, S. Grabowsky, D. Jayatilaka and M.A. Spackman, Accurate and Efficient Model Energies for Exploring Intermolecular Interactions in Molecular Crystals. *The Journal of Physical Chemistry Letters*, 5 (2014) 4249-4255.

[30] A.J. Edwards, C.F. Mackenzie, P.R. Spackman, D. Jayatilaka and M.A. Spackman, Intermolecular interactions in molecular crystals: what's in a name?. *Faraday Discussions,* 203 (2017) 93-112.

[31] V. Sangeetha, M. Govindarajan, N. Kanagathara, M.K. Marchewka, M. Drozd and G. Anbalagan, Vibrational, DFT, and thermal analysis of 2,4,6-triamino-1,3,5-triazin-1-ium 3-(prop-2-enoyloxy) propanoate acrylic acid monosolvate monohydrate. *Journal of molecular structure*, 1054-1055 (2013) 307-320.

[32] Ji Aihara, Weighted HOMO-LUMO energy separation as an index of kinetic stability for fullerenes. *Theoretical chemistry accounts,* 102 (1999) 134–138.

[33] S. Murugavel, S. Sundramoorthy, D. Lakshmanan, R. Subashini, P. Pavan Kumar, Synthesis, crystal structure analysis, spectral (NMR, FT-IR, FT-Raman and UV-Vis) investigations, molecular docking studies, antimicrobial studies and quantum chemical calculations of a novel 4-chloro-8-methoxyquinoline-2(1H)-one: an effective antimicrobial agent and an inhibition of DNA gyrase and lanosterol-14α-demethylase enzymes. *Journal of molecular structure*, 1131 (2017) 51-72.

HOW TO CITE THIS ARTICLE

Ruchika Sharma, Mulveer Singh, k. Kamal, Nitin G. Ghatpande, Mahidansha M. Shaikh, Jagannath S. Jadhav, Saminathan Murugavel, and Rajni Kant,Synthesis, crystal structure, Hirshfeld surface, crystal voids, energy frameworks, DFT and molecular docking analysis of (2,6-dimethoxyphenyl)acetic acid, Ad. J. Chem. B, 4 (2022) 1-16.

DOI: 10.22034/ajcb.2022.320258.1102

URL: http://www.ajchem-b.com/article_145346.html